MdMYB1 Regulates Anthocyanin and Malate Accumulation by Directly Facilitating Their Transport into Vacuoles in Apples[1][OPEN]

Da-Gang Hu, Cui-Hui Sun, Qi-Jun Ma, Chun-Xiang You, Lailiang Cheng, and Yu-Jin Hao*

State Key Laboratory of Crop Biology, National Research Center for Apple Engineering and Technology, College of Horticulture Science and Engineering, Shandong Agricultural University, Tai-An, Shandong 271018, China (D.-G.H., C.-H.S., Q.-J.M., C.-X.Y., Y.-J.H.); and Department of Horticulture, Cornell University, Ithaca, New York 14853 (L.C.)

ORCID ID: 0000-0003-1759-9761 (L.C.).

Tonoplast transporters, including proton pumps and secondary transporters, are essential for plant cell function and for quality formation of fleshy fruits and ornamentals. Vacuolar transport of anthocyanins, malate, and other metabolites is directly or indirectly dependent on the H^+-pumping activities of vacuolar H^+-ATPase (VHA) and/or vacuolar H^+-pyrophosphatase, but how these proton pumps are regulated in modulating vacuolar transport is largely unknown. Here, we report a transcription factor, MdMYB1, in apples that binds to the promoters of two genes encoding the B subunits of VHA, MdVHA-B1 and MdVHA-B2, to transcriptionally activate its expression, thereby enhancing VHA activity. A series of transgenic analyses in apples demonstrates that MdMYB1/10 controls cell pH and anthocyanin accumulation partially by regulating *MdVHA-B1* and *MdVHA-B2*. Furthermore, several other direct target genes of MdMYB10 are identified, including *MdVHA-E2*, *MdVHP1*, *MdMATE-LIKE1*, and *MdtDT*, which are involved in H^+-pumping or in the transport of anthocyanins and malates into vacuoles. Finally, we show that the mechanism by which MYB controls malate and anthocyanin accumulation in apples also operates in Arabidopsis (*Arabidopsis thaliana*). These findings provide novel insights into how MYB transcription factors directly modulate the vacuolar transport system in addition to anthocyanin biosynthesis, consequently controlling organ coloration and cell pH in plants.

In plant cells, the vacuole, which occupies most of the cell volume, plays a crucial role in generating turgor, storing metabolites and maintaining cell pH balance (Marty, 1999; Martinoia et al., 2007; Faraco et al., 2014). In the case of fleshy fruits, the function of the vacuole in the peel and flesh cells has direct implications for fruit quality because the vacuole stores a wide variety of compounds, such as sugars, organic acids, and secondary metabolites, the composition and concentrations of which largely determine the appearance (especially color), taste, and flavor of the fruits (Shiratake and Martinoia, 2007; Sweetman et al., 2009; Etienne et al., 2013).

On the vacuolar membrane, two distinct proton pumps, vacuolar H^+-ATPase (V-ATPase) and H^+-pyrophosphatase (V-PPase), drive vacuolar acidification by transporting protons across the tonoplast into the vacuole (Shiratake and Martinoia, 2007). Moreover, a large number of secondary transporters and channels on the tonoplast, such as malate transporters (tDT), the vacuolar malate channel ALMT9, MATE-type anthocyanin transporters, and ABC transporters, are responsible for transporting malate and anthocyanins from the cytosol into the vacuole, respectively (Emmerlich et al., 2003; Kovermann et al., 2007; Gomez et al., 2009; Francisco et al., 2013). The activities of these transporters are directly or indirectly dependent on the proton gradients generated by V-ATPase and V-PPase (Shiratake and Martinoia, 2007).

V-ATPase is a complicated complex that is composed of the peripheral subcomplex V_1 and the membrane-bound subcomplex V_0. V_1 has eight different subunits (from A to H) and is mainly responsible for ATP hydrolysis, while V_0 contains six subunits (VHA-a, -c, -c′, -c′′, -d, and -e) and is responsible for proton translocation (Padmanaban et al., 2004). Plant H^+-PPases are of two distinct types. Type I is K^+-sensitive, while type II is K^+-insensitive and Ca^{2+}-hypersensitive. These H^+-PPases generate proton gradients across the vacuolar membrane (Gaxiola et al., 2007). In flesh cells, vacuolar proton pumps and secondary transporters act together to transport a large amount of organic acids into the vacuole, thereby generating a low cell pH value via a so-called "acid trap" mechanism (Martinoia et al.,

[1] This work was supported by grants from Ministry of Science and Technology of China (2011AA100204), NSFC (31272142, 31325024, 31471854), Ministry of Education of China (IRT15R42), and Shandong Province (SDAIT-03-022-03).

* Address correspondence to haoyujin@sdau.edu.cn.

The author responsible for distribution of materials integral to the findings presented in this article in accordance with the policy described in the Instructions for Authors (www.plantphysiol.org) is: Yu-Jin Hao (haoyujin@sdau.edu.cn).

Y.-J.H. and D.-G.H. conceived and designed the experiments; D.-G.H., C.-H.S., Q.-J.M., and C.-X.Y. performed the experiments; D.-G.H., Y.-J.H., and L.C. wrote the article.

[OPEN] Articles can be viewed without a subscription.

www.plantphysiol.org/cgi/doi/10.1104/pp.15.01333

2007; Etienne et al., 2013), which contributes to the overall organoleptic quality of the fruits.

Organ color, an important economic trait in fruits and ornamental crops, is determined by various pigments. Among these pigments, anthocyanins are often responsible for organ coloration, such as bright red, red, blue, and violet (Młodzińska, 2009). Anthocyanins are biosynthesized via the flavonoid pathway in the cytosol and transported into the vacuole by putative anthocyanin transporters, such as MATE-type and ABC transporters (Debeaujon et al., 2001; Goodman et al., 2004; Marinova et al., 2007; Gomez et al., 2009). This biosynthetic pathway is transcriptionally regulated by an MBW complex containing WD-repeat proteins, bHLH, and MYB transcription factors, which are highly conserved among higher plant species (Koes et al., 2005; Ramsay and Glover, 2005; Ballester et al., 2010; Albert et al., 2011; Xie et al., 2012). Among them, MYB regulators are one of the master candidate genes regulating anthocyanin synthesis (Ban et al., 2007; Lin-Wang et al., 2010). In apples (*Malus domestica*), *MdMYBA*, *MdMYB1*, and *MdMYB10* are alleles of a single locus in different genotypes. They differ in a repeated sequence of the promoter region. This repeated sequence ensures high expression levels of *MdMYB10* in apple flesh and foliage. In contrast, *MdMYB1* and *MdMYBA* alleles lack such a repeated sequence in their promoters, and their expression is limited to apple peels (Mahmoudi et al., 2012). In fact, the MdMYB1 protein is exactly identical to MdMYBA (Takos et al., 2006) and shares 98% of its homology with MdMYB10 (Espley et al., 2007).

In addition to anthocyanin biosynthesis and transportation, cell pH shifts the anthocyanin absorption spectrum to change the hue of tissues and organs (Yoshida et al., 2009). On the plasma membrane, distinct P-type H^+-ATPases, such as PM H^+-ATPases, control the cytoplastic pH (Palmgren, 2001; Palmgren and Nissen, 2011). Meanwhile, vacuolar proton pumps and secondary transporters are responsible for the regulation of vacuolar pH (Verweij et al., 2008). In Japanese morning glory (*Ipomoea nil*), mutants of the vacuolar Na^+/H^+ exchangers, *InNhx1* and *InNhx2*, are unable to increase vacuolar pH and therefore develop purple reddish petals (Fukada-Tanaka et al., 2000; Ohnishi et al., 2005). In *Petunia*, the flower color generally varies from red to purple; however, seven mutants named *ph1* to *ph7* exhibit an increased vacuolar pH and produce bluish flowers (de Vlaming et al., 1983). In the past decade, most *PHs* genes have been identified and characterized. Among these genes, *PH1* and *PH5* encode vacuolar P_{3B}-ATPase and P_{3A}-ATPase, respectively (Verweij et al., 2008; Faraco et al., 2014). Both PH1 and PH5 contribute to vacuolar acidification (Verweij et al., 2008), and PH1 is a putative Mg^{2+} transporter. Although PH1 does not have proton transporter activity, it interacts with PH5 to boost the proton pump activity of PH5, thereby acidifying the cells (Faraco et al., 2014).

PH4 or AN2 (ANTHOCYANIN 2), which encodes an MYB transcription factor, interacts with the WD-repeat protein AN11 and bHLH transcription factor (TF) PH6/AN1 to intensify vacuolar acidification and control flower color in *Petunia* petal cells (Koes et al., 2005; Quattrocchio et al., 2006; Faraco et al., 2014). The loss-of-function mutant *ph4* exhibits a bluish flower color due to the increased pH in the petal cells, while *AN2* expression driven by a *35S* promoter rescues pigmentation of *an2* petals from white to a bluish color (Quattrocchio et al., 2006; Quattrocchio et al., 2013). It has recently been shown that *PH1* and *PH5* are transcriptionally activated by the AN11-PH6/AN1-PH4 complex (Faraco et al., 2014), suggesting a potential link between vacuolar acidification and anthocyanin accumulation. However, the exact mechanism of this transcriptional regulation has not been identified. In addition, it is not known whether other genes involved in the vacuolar transport of metabolites are transcriptionally regulated by the same complex. We hypothesized that the MYB transcriptional factor for anthocyanin synthesis also directly regulates V-ATPase and possibly other vacuolar transporters in coordinating vacuolar acidification and the transport of anthocyanins and other metabolites.

Remarkably, anthocyanins and malate, which are synthesized in the cytosol, translocate to various cell compartments, especially to the vacuoles, in apples (Fernie and Martinoia, 2009; Li et al., 2012; Etienne et al., 2013). The biosynthesis of anthocyanin is transcriptionally regulated by an MYB-bHLH-WDR (MBW) complex, such as MdTTG1-MdbHLH3-MdMYB1 in apples (An et al., 2012; Li et al., 2012; Xie et al., 2012; Vimolmangkang et al., 2013; An et al., 2015). However, the *MdtDT* gene is cloned, and preliminary work suggests that it plays a role in malate transport into the vacuole in apples (Yao et al., 2011b). In addition, the *Ma* locus is a major QTL that controls variations in the flesh and juice acidity levels (Xu et al., 2012). Recent genetic analysis indicates that two ALMT-like genes, *Ma1* and *Ma2*, are strong candidates for the *Ma* locus (Bai et al., 2012).

In this study, we show that apple MdMYB1/10 TF directly regulates the expression of several genes that encode vacuolar proton pump subunits, including *MdVHA-B1*, *MdVHA-B2*, *MdVHA-E2*, and *MdVHP1*; an anthocyanin transporter, *MdMATE-LIKE1*; an ABC transporter; and a malate transporter, *MdtDT*, in modulating anthocyanin/malate accumulation and cell pH. We also demonstrate that the mechanism through which MYB TF controls cell pH and the vacuolar accumulation of anthocyanins and malate is conserved between apples and Arabidopsis (*Arabidopsis thaliana*).

RESULTS

Identification of the MYB Transcription Factor Binding to the cis-Element of *MdVHA-B1* Promoter

By sequence analysis, we found a typical MYB-binding cis-element present in the promoter region of the V-ATPase subunit gene *MdVHA-B1* (Fig. 1A). To

identify the potential MYB proteins that recognize and bind to the MYB cis-element, an oligonucleotide probe, ACAATCAACGGTTAAA, from the *MdVHA-B1* promoter, which contains the typical MYB cis-element CAACGG, was used for DNA-affinity trapping and electrophoretic mobility shift assays (EMSAs). When the nuclear protein extracts were incubated with biotin-labeled *MdVHA-B1* promoter oligonucleotides, a DNA-protein complex with a slower mobility in EMSA was observed (Fig. 1, B and C).

Subsequently, a mass spectrometry analysis was performed to identify the proteins that bind to the oligonucleotide. Interestingly, the protein MdMYB1 is a candidate in the LC/MS data (Supplemental Appendix S1). *MdMYB1* and its alleles, *MdMYB10* and *MdMYBA*, are master regulators for anthocyanin biosynthesis in apples (Takos et al., 2006; Ban et al., 2007; Li et al., 2012).

MdMYB1 Binds to the Promoters of *MdVHA-B1* and *MdVHA-B2*

To determine whether MdMYB1 binds to the MYB recognition site in the *MdVHA-B1* promoter, EMSA was performed using prokaryon-expressed and purified MdMYB1-GST fusion proteins. A specific DNA-MdMYB1 protein complex was detected when the CAACGG-containing oligonucleotide was used as a labeled probe (Fig. 2A). The formation of these complexes was reduced with increasing amounts of the unlabeled MYB competitor probe with the same sequence. This competition was not observed when using a mutated version of the probe (Fig. 2A). The specificity of this competition confirms that the specific binding of MdMYB1 to *MdVHA-B1* promoter requires the MYB recognition sequence.

In apples, there are three isoforms of V-ATPase subunit B (VHA-B) of the V_1 complex. They are encoded by three genes: *MdVHA-B1*, *MdVHA-B2* and *MdVHA-B3* (Supplemental Fig. S1). Our sequence analysis showed that all three *MdVHA-Bs* contain MYB recognition sites in their promoter regions. EMSA demonstrated that the MdMYB1 protein binds to the promoters of *MdVHA-B1* and *MdVHA-B2*, but not to that of *MdVHA-B3* (Fig. 2, A–C; Supplemental Fig. S2, A and B).

To verify in vivo binding of MdMYB1 to the *MdVHA-B1* and *MdVHA-B2* promoters, ChIP-PCR assays were conducted using *35S::MYB1-GFP* and *35S::GFP* transgenic apple calli, respectively. The MYB-element-containing promoter regions of *MdVHA-B1* and *MdVHA-B2*, but not *MdVHA-B3*, were enriched by ChIP in the *35S::MYB1-GFP* transgenic calli compared to the *35S::GFP* control (Fig. 2D). These results provide in vivo evidence for the binding of MdMYB1 to the *MdVHA-B1* and *MdVHA-B2* promoters.

GUS assays were then used to confirm the activation of MdMYB1 through the *MdVHA-B1* and *MdVHA-B2* promoters using the *GUS* reporter gene. Three recombinant plasmids, $P_{MdVHA\text{-}B1}$*::GUS*, $P_{MdVHA\text{-}B2}$*::GUS*, and $P_{MdVHA\text{-}B3}$*::GUS*, were combined with *35S::MdMYB1* and genetically transformed into apple calli (Fig. 2E; Supplemental Fig. S3, A and B). The transgenic-calli-containing $P_{MdVHA\text{-}B1}$*::GUS* (or $P_{MdVHA\text{-}B2}$*::GUS*) plus *35S::MdMYB1* exhibited a much higher GUS activity than those harboring $P_{MdVHA\text{-}B1}$*::GUS* (or $P_{MdVHA\text{-}B2}$*::GUS*) alone. In contrast, the addition of *35S::MdMYB1* had little influence on the GUS activity in $P_{MdVHA\text{-}B3}$*::GUS* transgenic calli, indicating that MdMYB1 activates *GUS* transcription driven by the promoters of *MdVHA-B1* (or *MdVHA-B2*), but not by that of *MdVHA-B3*.

MdMYB1 Modulates Anthocyanin and Malate Accumulation, As Well As Cell pH Partially via *MdVHA-B1* and *MdVHA-B2*

To characterize the functions of *MdMYB1* and *MdVHA-Bs*, the full-length sense ORFs and antisense cDNA fragments of *MdMYB1* and *MdVHA-Bs* were used to construct expression vectors. A total of five

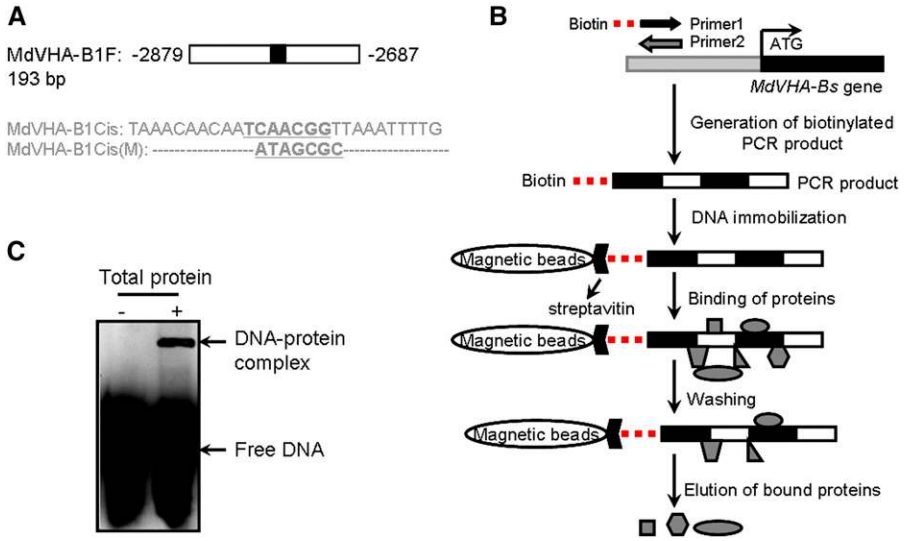

Figure 1. Identification of the MYB transcription factors binding to the cis-element of the *MdVHA-B1* promoter. A, The putative MdMYB1 TF-binding element on the *MdVHA-B1* promoter. The black box represents the MdMYB1-binding motif. B, Schematic outline of the method used for the affinity trapping of DNA-binding proteins. C, Identification of the MYB TF proteins binding to the cis-element of the *MdVHA-B1* promoter with EMSA. The positions of the free DNA probes and DNA-protein complexes are indicated by arrows. + and − represent with or without the addition of total protein extracted from apple plants, respectively.

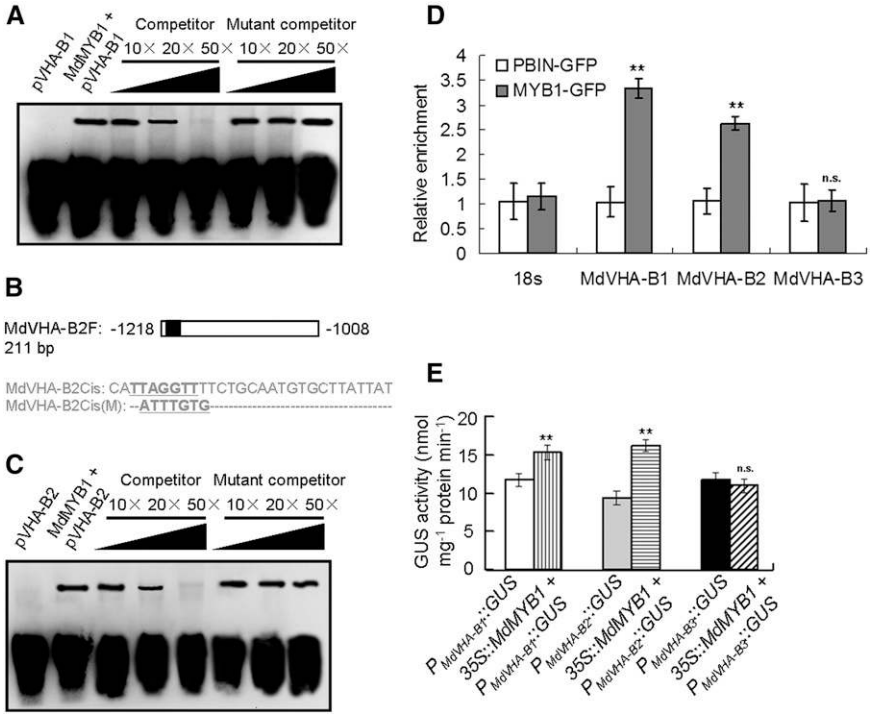

Figure 2. MdMYB1 specifically binds to the promoters of *MdVHA-B1* and *MdVHA-B2*. A, Interaction of the MdMYB1 protein with labeled DNA probes for the cis-elements of the *MdVHA-B1* promoter in the EMSA. *pVHA-B1* is used as a negative control without the MdMYB1 protein. B, The cis-element sequences and positions of the oligonucleotides within the *MdVHA-B2* promoter that was used for the EMSAs. C, EMSA verification of the interaction between the MdMYB1 protein and the cis-element of the *MdVHA-B2* promoter. D, The relative enrichment of the *MdVHA-B1*, *MdVHA-B2* and *MdVHA-B3* promoter fragments. The MdMYB1-DNA complex was coimmunoprecipitated from *MdMYB1-GFP* transgenic apple calli using an anti-GFP antibody. PBIN-GFP was used as a negative control. E, GUS activity in the transgenic apple calli as labeled. The means and standard deviations were calculated from the results of three independent experiments.

types of *35S*-driven vectors of MdMYB1-S ("S" means sense), MdMYB1-AS ("AS" means antisense), MdVHAB1-S and MdVHABs-AS (antisense for both MdVHA-B1 and MdVHA-B2) were made. Subsequently, eight single and combinations of plasmid vectors, i.e. empty vector control, MdMYB1-S, MdVHAB1-S, MdMYB1-S+MdVHAB1-S, MdMYB1-S+MdVHABs-AS, MdMYB1-AS, MdVHABs-AS, and MdMYB1-AS +MdVHABs-AS, were used for genetic transformation. Because it is very difficult to generate transgenic plants in apples, especially for those containing two recombinant plasmids together, apple calli were used for genetic transformation and functional characterization.

As a result, eight transgenic apple calli were obtained, as indicated in Figure 3A. The qPCR assays demonstrated that the overexpression of the *MdMYB1* gene enhanced the transcript levels of *MdVHA-B1* and *MdVHA-B2,* but not that of *MdVHA-B3*, compared with the wild-type control (Fig. 3B), suggesting a positive regulation of MdMYB1 to *MdVHA-B1* and *MdVHA-B2* genes. Meanwhile, an anti-MdVHAB antibody, which is specific to MdVHA-B1 and MdVHA-B3, but not to MdVHA-B2 (Supplemental Fig. S1B), was used for immunoblotting assays. The abundance of MdVHA-B1 increased with MdMYB1 protein levels, whereas MdVHA-B3 remained at a similar level in the control and transgenic apple calli (Fig. 3C). To examine whether MdMYB1 positively regulates MdVHA-B2 at the protein level, two transgenic apple calli, i.e. $P_{MdVHA-B2}$*::MdVHA-B2-GUS* (transgenic calli containing *MdVHA-B2-GUS* fusion gene driven by *MdVHA-B2* promoter) and *35S::MdMYB1* +$P_{MdVHA-B2}$*::MdVHA-B2-GUS* (*MdMYB1* overexpressor in a $P_{MdVHA-B2}$*::MdVHA-B2-GUS* background), were obtained. The results showed that the abundances of MdVHA-B1 and MdVHA-B2-GUS proteins were positively regulated by MdMYB1, while that of MdVHA-B3 was not (Supplemental Fig. S4). Therefore, MdMYB1 acts upstream of MdVHA-B1 and MdVHA-B2 to activate their transcript levels and protein abundances in apple calli.

In apples, MdbHLH3 binds to the promoter of *MdMYB1* to activate its transcription (Xie et al., 2012). As a result, transgenic apple plants overexpressing *MdbHLH3* generated more transcripts of the *MdMYB1* gene, which subsequently promoted the expression of *MdVHA-B1* and *MdVHA-B2* genes, thereby exhibiting a much higher malate content and a lower cell pH than the wild-type control (Supplemental Fig. S5, A–C). In addition, *MdMYB9* is involved in anthocyanin biosynthesis (An et al., 2015), while *MdoMYB121* is involved in abiotic stress tolerance (Cao et al., 2013). Their overexpression did not influence the expression of *MdVHA-Bs* genes, suggesting that not all MYB TFs affect the regulation of V-ATPase subunits (Supplemental Fig. S5, D and E).

MdMYB1 is a major regulator of anthocyanin biosynthesis (Takos et al., 2006). Its overexpression noticeably influenced anthocyanin accumulation in transgenic apple calli (Fig. 3, A and D), indicating that *MdMYB1* successfully functions in these transgenic calli. Subsequently, the V-ATPase hydrolysis activities, H^+ transport activities, and malate contents were determined. Before the determination of V-ATPase activity, we detected the purity of vacuolar membranes isolated from wild-type apple plants. The results showed that the tonoplast fraction was

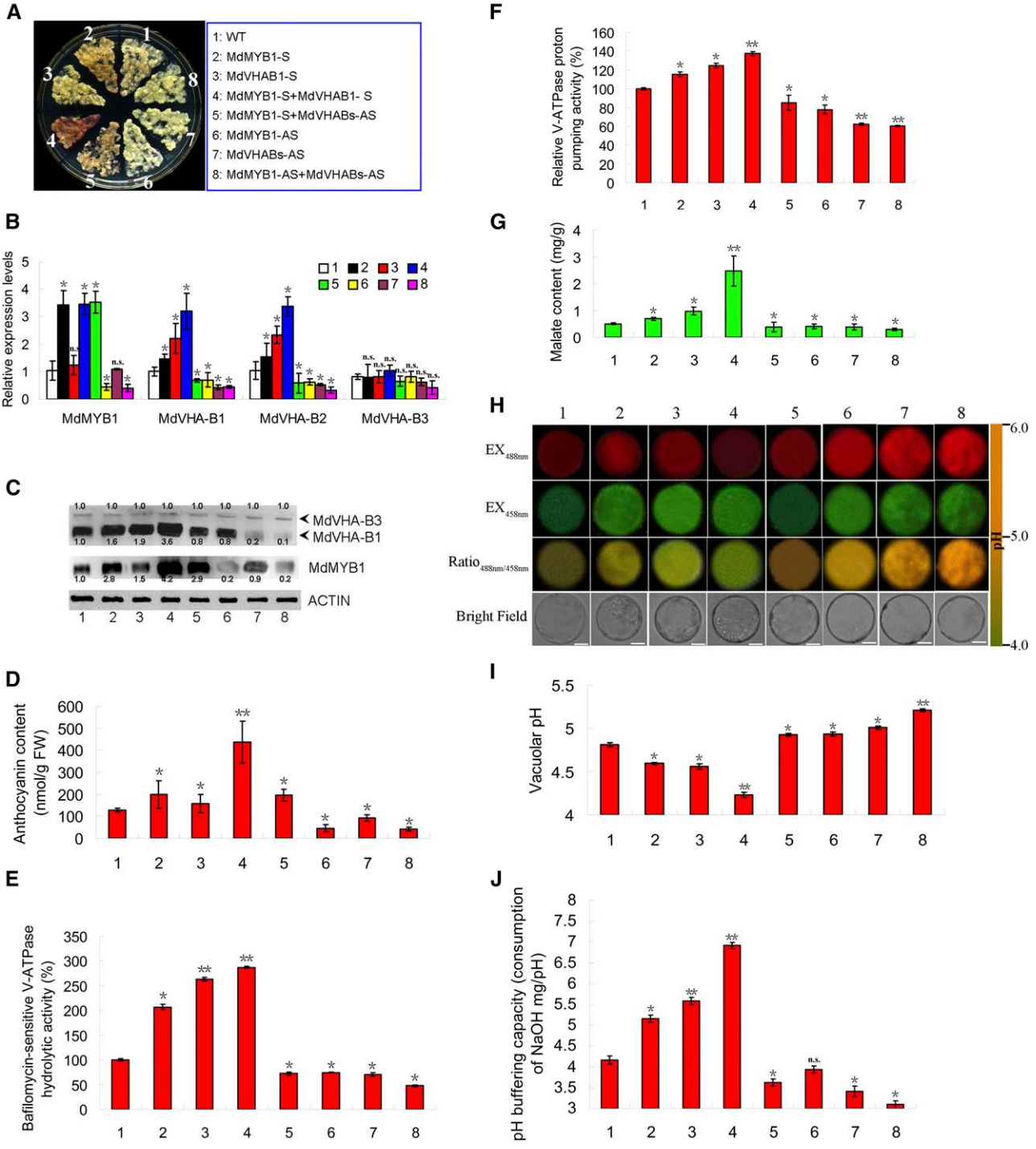

Figure 3. MdMYB1 controls malate and anthocyanin accumulation and cell pH via *MdVHA-B1* and *MdVHA-B2* in apple calli. A, Anthocyanin accumulation in wild-type and transgenic apple calli under 17°C plus UVB light conditions. The numbers 1 to 8 represent the wild-type and transgenic apple calli containing different combinations of constructs as indicated. B and C, qRT-PCR (B) and western blotting (C) analyses of MdMYB1 and MdVHA-Bs transcripts/proteins in the wild-type and transgenic apple calli. All protein amounts were normalized based on the protein folds of the wild-type control. Note: In C, protein bands were quantified by scanning densitometry using a Hewlett Packard scanjet scanner and Scanplot software. All protein amounts were normalized based on the protein folds of the wild-type control. D, Anthocyanin content in the wild-type and transgenic apple calli. E, Bafilomycin A_1-sensitive ATP hydrolytic activity of V-ATPase vacuolar membrane vesicles were isolated from plant cells, including wild-type and transgenic apple calli. After preincubation in the presence and absence of bafilomycin A_1, ATP was added as a substrate to start the reaction. Hydrolytic activity was assayed for 30 min. The reaction was stopped by the addition of

highly pure, with strong enrichment of vacuolar markers (Supplemental Fig. S6, A and B), and can be used for the further determination of V-ATPase activity. The results demonstrated that MdMYB1 controlled V-ATPase activity and malate contents, which was partially, if not completely, dependent on *MdVHA-B1* and *MdVHA-B2* in apple calli (Fig. 3, E–G).

The transport of H^+ into vacuoles contributes to the acidification of vacuolar compartments and the establishment of pH gradients across tonoplasts (Gaxiola et al., 2007). To assess the effects of V-ATPase activities on vacuolar pH, the rationmetric fluorescent pH indicator 2′,7′-bis-(2-carboxyethyl)-5-(6)-carboxyfluorescein (BCECF) was used to measure vacuolar pH (Swanson and Jones, 1996). The pH values were calculated from fluorescence ratios of confocal images (Fig. 3H) based on an in situ calibration curve (Supplemental Fig. S7). As a result, the average vacuolar pH was 4.81 in wild-type apple calli, but the pH of the *MdMYB1* and *MdVHA-B1* overexpressors shifted to 4.59 and 4.56, respectively (Fig. 3, H and I). Notably, MdMYB1-S+MdVHAB1-S and MdMYB1-AS+MdVHABs-AS apple calli were significantly shifted to 4.23 and 5.21, respectively (Fig. 3, H and I). Hence, a higher luminal H^+ concentration in *MdMYB1* and *MdVHA-B1* overexpressors, as indicated by the lower pH values, further supports that MdMYB1 and MdVHA-B1 are required to maintain tonoplast V-ATPase activity.

Furthermore, the pH buffering capacities of wild-type and transgenic apple calli were also determined. The results showed that *MdMYB1* and *MdVHA-B1* overexpressors have a higher pH buffering capacities compared with WT apple calli (Fig. 3J), further supporting that MdMYB1 controls vacuolar pH, which is dependent on *MdVHA-B1* and *MdVHA-B2* in apple calli.

Subsequently, a viral vector-based method was used to verify the functions of MdMYB1 and MdVHA-Bs in regulating coloration and acidity in apple fruits and petals. The results showed that MdMYB1 positively activates *MdVHA-B1* and *MdVHA-B2*, thereby increasing the malate contents and decreasing the cell pH in apple fruits and red-flesh apple petals, just as it did in the apple calli (Fig. 3; Supplemental Fig. S8). In addition, the ectopic expression of *MdMYB1* or *MdVHA-B1* not only promoted anthocyanin accumulation but also enhanced malate contents in transgenic tobacco flowers (Supplemental Fig. S9).

MdMYB10 Influences the Flesh Acidity and Color in Red-Flesh Apples

In apples, *MdMYB1*, *MdMYB10*, and *MdMYBA* are allelic to each other (Ban et al., 2007; Lin-Wang et al., 2010). Compared to *MdMYB1* and *MdMYBA*, the *MdMYB10* locus is dominant and constitutively generates an extremely high level of *MdMYB10* transcript and protein, thereby making the tree produce red leaves and red flesh fruits (Espley et al., 2007, 2009; Lin-Wang et al., 2010). To verify whether MdMYB10 regulates *MdVHA-B1* and *MdVHA-B2*, in this study, two heterozygous red-flesh apple genotypes were sexually crossed, generating hybrid seeds.

After germination, the hybrid population was divided into red-leaf and green-leaf seedlings (Supplemental Fig. S10A). Subsequently, 10 red-leaf and 10 green-leaf seedlings were randomly chosen for further investigation. Expression and western blotting analyses demonstrated that the red-leaf seedlings produced higher levels of MdVHA-B1 and MdVHA-B2, but not MdVHA-B3, than the green-leaf ones (Supplemental Fig. S10A). At the same time, the red-leaf seedlings produced more anthocyanins and malate while exhibiting a lower pH value than the green-leaf ones (Supplemental Fig. S10, B–D).

The red-leaf trees produced red-flesh fruits, while the green-leaf trees produced non-red-flesh fruits (Fig. 4A). Five trees per flesh color type were chosen. These trees exhibited similar fruit development and ripening stages. The fruits were taken at 30, 90, and 120 d after bloom (DAB) for characterization. qPCR and western blotting analyses demonstrated that the red-flesh fruits produced more MdMYB10 transcript and protein, and consequently more MdVHA-B1 and MdVHA-B2, but not MdVHA-B3, than the non-red-flesh fruits (Fig. 4, B

Figure 3. (*Continued.*)
trichloroacetic acid. The samples were extracted with chloroform to remove lipids and detergents. After centrifugation, the upper aqueous phase was transferred to clean test tubes and incubated with buffers containing ascorbic acid and ammonium molybdate. The concentration of inorganic phosphate was measured by a spectrophotometer at 700 nm and converted to the rate of ATP hydrolysis. F, Proton-pumping activity of V-ATPase was measured by tracking the ATP-dependent quenching of acridine orange using a fluorescence spectrometer with excitation at 493 nm and emissions at 545 nm. Purified vacuolar membrane vesicles were resuspended in 25 mM Tris (pH 7.2), 25 mM KCl, 5 mM acridine orange, and 5 mM $MgCl_2$ in the presence and absence of bafilomycin A_1. ATP was added at a final concentration of 5 mM to initiate transport. The proton transport rate was determined as the slope of the quench that gave a linear response during the first 10 s immediately after the addition of ATP. G, Malate content in the wild-type and transgenic apple calli. H, The images show emission intensities of protoplast vacuoles in apple calli loaded with BCECF at 488 nm (the first column, red) and 458 nm (the second column, green). The ratio images indicate an increased or decreased vacuolar pH in transgenic apple calli compared to wild type (the third column). Pseudo-color scale on the right indicates the intensity of the fluorescence, in which yellow and red represent the minimum and maximum intensity, respectively. Scale bar = 10 μm. I, Quantification of the luminal pH in wild-type and transgenic apple calli vacuoles. Bars represent SE of 30 measurements from 10 different intact vacuoles. J, pH buffering capacities in the wild-type and transgenic apple calli. In B to G and I to J, data are shown as the mean ± SE, which were analyzed based on more than nine replicates. Statistical significance was determined using Student's *t* test in different apple calli lines. n.s., $P > 0.01$; $^*P < 0.01$; $^{**}P < 0.001$.

and C). As a result, the red-flesh fruits exhibited higher V-ATPase activity, accumulated more malate, and showed a lower pH than the nonred ones (Fig. 4, D–G).

To rule out the possible involvement of segregating factors other than *MdMYB10* locus to the greatest extent, another hybridization population from a sexual cross between a red flesh genotype, "Jinshanyilamu," and a non-red flesh genotype, "Yepingguo," was used. The results further verified the role of the *MdMYB10* locus in regulating V-ATPase activity, anthocyanin, and malate content (Supplemental Fig. S11).

MdMYB10 Modulates Malate Accumulation and Cell pH by Activating More Genes Than *MdVHA-Bs*

To determine whether MdMYB10 regulates genes other than *MdVHA-Bs*, total RNAs were extracted from fruit samples taken from five trees per flesh color type at

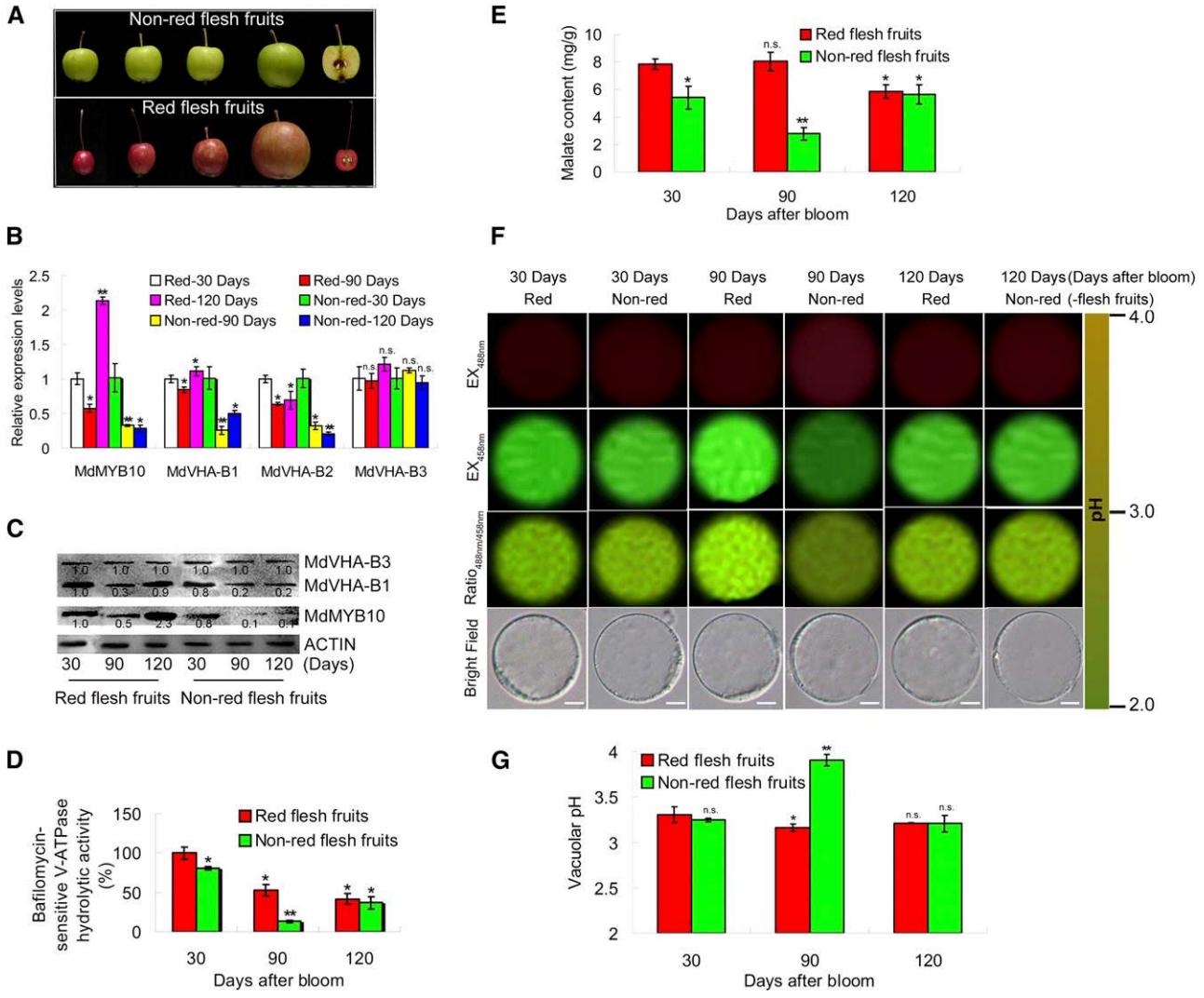

Figure 4. MdMYB10 promotes malate accumulation and cell acidification in red-flesh apples. A, Photos of fruits that were harvested from red- and non-red-flesh hybrid trees. B and C, Transcript level (B) and protein abundance (C) of MdMYB10/MdVHA-Bs in the red-flesh and non-red-flesh fruits at 30, 90, and 120 DAB. Note: In C, protein bands were quantified by scanning densitometry using a Hewlett Packard scanjet scanner and Scanplot software. All protein amounts were normalized based on the protein folds of the 30 DAB samples. D and E, The V-ATPase hydrolytic activity (D) and malate content (E) in these two types of apple fruits. F, The images show emission intensities of protoplast vacuoles in apple fruits loaded with BCECF at 488 nm (first column, red) and 458 nm (second column, green). The ratio images indicate an increased or decreased vacuolar pH in red flesh apple fruits compared with non-red flesh apple fruits (the third column). The pseudo-color scale on the right indicates the intensity of the fluorescence, in which yellow and red represent the minimum and maximum intensity, respectively. Bar = 10 μm. G, Quantification of the luminal pH in the vacuoles of red flesh and non-red flesh apple fruits. Error bars represent SE of 30 measurements from 10 different intact vacuoles. In B, D, E, and G, data are shown as the mean ± SE, which were analyzed based on more than five trees bearing red- or non-red-flesh fruits. Statistical significance was determined using Student's *t* test in the red and non-red-flesh fruits. n.s., $P > 0.01$; *$P < 0.01$; **$P < 0.001$.

the stage of 90 DAB for an RNA-seq analysis. At least 20,000,000 sequence reads were generated, each 100 to 150 bp in length, encompassing 2.2 Gb of sequence data, which was sufficient to quantitatively analyze the gene expression. A total of 40,271 genes were detected. Among these genes, 3938 were up-regulated and 3725 genes were down-regulated in the red-fleshed compared to the non-red-fleshed apple fruits (Fig. 5A).

To facilitate the global analysis of the gene expression profiles and evaluate the anthocyanin- and malate-related genes that showed significant transcriptional changes in the above samples, a Gene Ontology (GO)-based classification was conducted by subjecting the sequences to InterPro and GO annotations. These annotations revealed that the absolute expression value (log2Ratio) of *MdMYB10* in the red-fleshed compared to the non-red-fleshed fruits was 6.45-fold, based on the FDR < 0.01, while the GO functional classification analysis of V-ATPase, V-PPase, malate synthetic, and transporter genes showed that most of these genes were up-regulated (Supplemental Appendix S2 and Supplemental Table S1). To test the accuracy of the RNA-Seq analysis, quantitative real-time PCR (qPCR) was performed on selected genes, including V-ATPase, V-PPase, malate related-genes (*MdcyMDH*, *MdmMDH*, *MdcyME*, *MdPEPCK*, and *MdPEPC*), anthocyanin synthesis-related genes (*MdANR*, *MdANS*, *MdCHI*, *MdCHS*, *MdFLS*, and *MdUFGT*) and vacuolar transporters and channels-related genes (*MdMATE-LIKE1*, *MdMATE-LIKE2*, *MdMATE-LIKE3*, *ABC transporter*, *MdALMT9*, and *MdtDT*) (Supplemental Appendix S3). The transcript level of most of these genes was increased, except for that of the malate channel *MdALMT9* gene (Fig. 5, B–D), which confirms the results of the RNA-Seq analysis.

To determine whether MdMYB1/10 directly regulates these genes, ChIP-PCR (in vivo) was performed. MdMYB1 directly bound to the cis-element of *MdVHA-E2*, *MdVHP1*, *MdMATE-LIKE1*, *ABC transporter*, and *MdtDT*, in addition to *MdVHA-B1* and *MdVHA-B2*, while other genes were the indirect target genes of MdMYB1/10 (Fig. 5E). Therefore, MdMYB1 mediates apple coloration

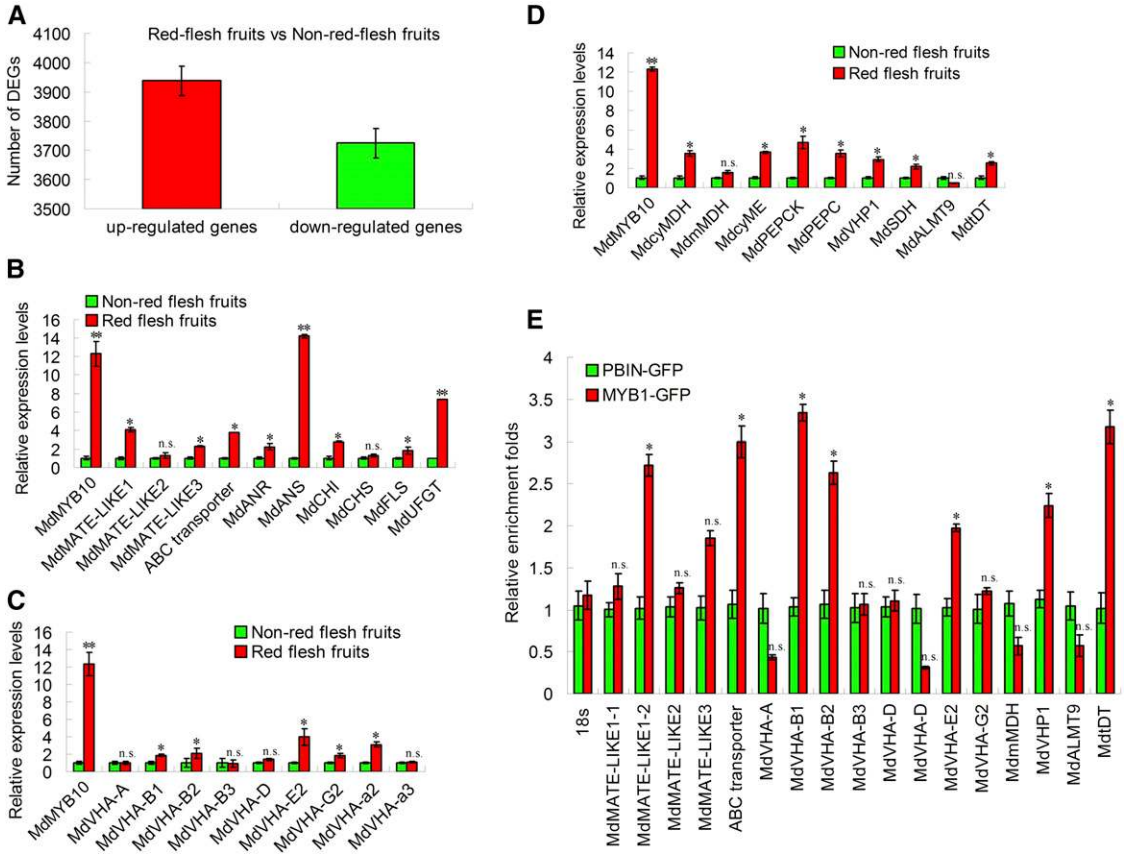

Figure 5. Identification of the target genes of MdMYB1/10. A, Number of up-regulated and down-regulated genes in the red-flesh fruits compared with non-red-flesh fruits with RNA-seq. B to D, The relative expression levels of genes involved in anthocyanin transport and biosynthesis (B), V-ATPase subunit genes (C), and genes involved in malate synthesis and transport (D) in red-flesh and non-red-flesh apple fruits. The fruits were sampled at 90 DAB. E, ChIP-qPCR assays of the enrichments of the target gene promoters in the *35S::MdMYB1-GFP* transgenic callus compared to the *35S::GFP* transgenic calli. Note: MATE-LIKE1-1 and MATE-LIKE1-2 represent cis-elements 1 and 2 in the promoters of *MATE-LIKE1* gene, respectively. In B to E, data are shown as the mean ± SE, which were analyzed based on more than nine replicates. Statistical significance was determined using Student's *t* test in different apple calli lines. n.s., $P > 0.01$; $^{*}P < 0.01$; $^{**}P < 0\ 0.001$.

and acidity by directly and indirectly regulating the expression of anthocyanin- and malate-related genes.

AtPAP1, a Master Regulator for Anthocyanin Biosynthesis, Also Modulates Malate Levels and Cell pH in Arabidopsis

In Arabidopsis, *PAP1* is homologous to apple *MdMYB1* and *MdMYB10* (Allan et al., 2008; Ban et al., 2007; Lin-Wang et al., 2010). Here, two *35S::PAP1-GFP* transgenic lines (*AtPAP1-GFP-1* and *AtPAP1-GFP-2*) and one T-DNA activation-tagged gain-of-function mutant, *AtPAP1-D,* were used to determine whether PAP1 functions similarly to MdMYB1/10 in Arabidopsis. The two transgenic lines and the mutant *AtPAP1-D* accumulated much more anthocyanin than the wild type, and the empty vector *pRI-GFP* control (Fig. 6, A–C).

To determine whether in vivo AtPAP1 binds to the promoters of the *AtVHA-B1*, *AtVHA-B2*, *AtVHA-B3*, *AtVHA-D*, *AtAVP1*, *AtMATE*, *AtABCB27*, *AtALMT9*, and *AttDT* genes, *35S::PAP1-GFP* (*AtPAP1-GFP-1*) and *35S::pRI-GFP* (*GFP* control) transgenic Arabidopsis plants were used for immunoprecipitation with the anti-GFP antibody. The enrichment of the promoters was detected with qPCR assays. The promoter regions of *AtVHA-B1*, *AtVHA-B2*, *AtAVP1*, *AtABCB27*, *AtMATE*, and *AttDT* containing the putative MYB cis-elements were enriched by ChIP in *AtPAP1-GFP-1* transgenic Arabidopsis compared to the *GFP* control, while the promoter regions of the other genes did not (Fig. 6D). These results further provide in vivo evidence for the specific binding of AtPAP1 to the *AtVHA-B1*, *AtVHA-B2*, *AtAVP1* (homologous to apple *MdVHP1*), *AtABCB27*, *AtMATE*, and *AttDT* promoters, thereby directly mediating the transcriptional activation of these genes. As a result, the malate content was much higher, while the cell pH was lower in the *AtPAP1* overexpression lines and the mutant *AtPAP1-D* than in the control (Fig. 6, E–G). Therefore, the mechanism through which MYB TF controls cell pH and coloration via the regulation of vacuolar proton pumps and malate- and anthocyanin-related transporters is conserved in different species.

DISCUSSION

MdMYB1 Links Vacuolar Acidification and Anthocyanin Accumulation by Activating Vacuolar Proton Pumps and Secondary Transporters

Acidification of the vacuole by proton pumps (V-ATPase and V-PPase) and vacuolar transport of metabolites by tonoplast transporters are important not only for proper cell function (Martinoia et al., 2007; Kovermann et al., 2007; Gomez et al., 2009) but also for quality formation of fleshy fruits and ornamental crops (Lobit et al., 2006; Shiratake and Martinoia, 2007; Etienne et al., 2013). Therefore, it is of considerable interest to understand how the genes encoding these proton pumps and transporters are transcriptionally modulated by TFs. In this study, we found that apple MdMYB1/10 TF and its Arabidopsis counterpart, AtPAP1, which are master regulators of anthocyanin biosynthesis (Espley et al., 2007; Li et al., 2012; Qiu et al., 2014), directly activate the expression of the genes encoding V-ATPase subunits, V-PPase, the anthocyanin transporter *MATE-LIKE1*, ABC transporter, and the malate transporter *tDT*. This clearly indicates that MYB transcriptional factors play a key regulatory role in vacuolar acidification and in the transport of anthocyanins and malate.

The direct interaction between MdMYB1 and the promoters of genes encoding V-ATPase subunits *MdVHA-B1* and *MdVHA-B2* is supported by both in vitro binding demonstrated by EMSA (Fig. 2, A and C) and in vivo binding in ChIP-PCR assays and GUS assays of the transgenic calli (Fig. 2, D and E). This transcriptional activation of both *MdVHA-B1* and *MdVHA-B2* leads to increases in V-ATPase activity (Fig. 3, E and F) and elevated cell acidification (Fig. 3, H and I). It has been demonstrated in other plant species that the overexpression of a single subunit of V-ATPase improves the expression of other subunits and ultimately increases overall V-ATPase activity (Keenan Curtis and Kane, 2002; Zhao et al., 2009), and our data are in line with these previous findings (Fig. 3, E and F; Supplemental Fig. S12). The higher V-ATPase activities and corresponding lower pH values detected in the red-flesh fruits relative to nonred fruits (Fig. 4, D, F, and G; Supplemental Fig. S11, D, E, and G) and apple fruits transiently overexpressing *MdMYB1* (Supplemental Fig. S8, D and F) confirm that MdMYB1 regulates flesh acidification primarily via the transcriptional activation of V-ATPase. In addition, our work shows that MdMYB1 also binds to the promoter of *MdVHP1* to regulate its expression (Fig. 5, D and E). It has been shown that ectopic and transient expression of the apple V-PPase gene *MdVHP1* promotes malate and anthocyanin accumulation in tomato fruits and grape berries, respectively (Y.X. Yao and Q.L. Dong, unpublished data). These results suggest that *MdVHP1* also contributes to cell acidification in *MdMYB1* and *MdMYB10* transgenic materials.

Although none of the transporters identified for vacuolar transport of anthocyanins (MATE-LIKE and ABC transporter) directly or indirectly use proton gradients in transporting anthocyanins from the cytosol into the vacuole (Gomez et al., 2009; Francisco et al., 2013), our data indicate that vacuolar acidification caused by the overexpression of subunit *MdVHA-B1* alone leads to the accumulation of anthocyanins in apple calli (Fig. 3, D, H, and I), apple fruits and petals (Supplemental Fig. S8, B, F, and H), and tobacco flowers (Supplemental Figure S9, C and E). This increased accumulation of anthocyanins, which primarily occurs in the vacuole, can be partially explained by the elevated expression of *MdMATE-LIKE1,* as demonstrated in the transgenic calli overexpressing *MdVHA-B1* (Supplemental Fig. S13). As anthocyanins must be synthesized first before being transported into the vacuole, these results also suggest a close relationship between vacuolar acidification and anthocyanin synthesis. This relationship is supported

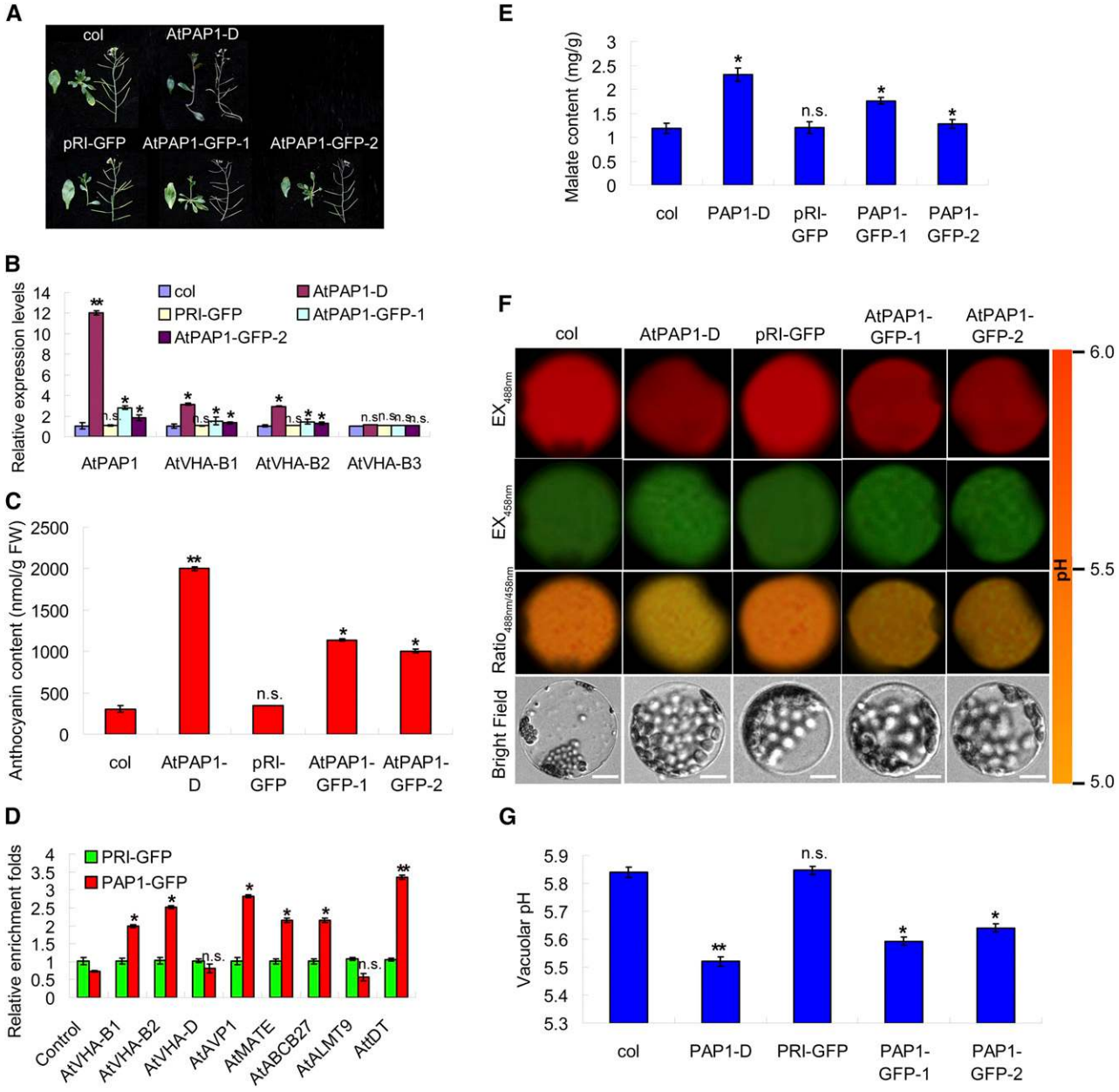

Figure 6. MYB TF AtPAP1 controls malate accumulation and cell acidification. A, Overexpression of *PAP1* and its gain-of-function mutant *AtPAP1-D* promote anthocyanin accumulation. Col., The wild-type background; *pRI-GFP*, empty vector; *AtPAP1-GFP-1* and *AtPAP1-GFP-2*, two overexpression lines containing the *AtPAP1-GFP* fusion gene under the control of the *35S* promoter; *AtPAP1-D*, a gain-of-function mutant of *AtPAP1* with enhanced anthocyanin accumulation in plants. B, The relative expression level of *AtPAP1* in Col., *pRI-GFP*, *AtPAP1-GFP-1*, *AtPAP1-GFP-2*, and *AtPAP1-D Arabidopsis*. C, Anthocyanin contents in Col., *pRI-GFP*, *AtPAP1-GFP-1*, *AtPAP1-GFP-2*, and *AtPAP1-D Arabidopsis*. D, ChIP-qPCR assays of the relative enrichment of the target gene promoters in *35S::AtPAP1-GFP* transgenic Arabidopsis compared to *35S::GFP* transgenic Arabidopsis. E, Malate content in Col., *PRI-GFP*, *AtPAP1-GFP-1*, *AtPAP1-GFP-2*, and *AtPAP1-D Arabidopsis*. F, The images show emission intensities of protoplast vacuoles in Arabidopsis loaded with BCECF at 488 nm (first column, red) and 458 nm (second column, green). The ratio images indicate an increased or decreased vacuolar pH in *AtPAP1* transgenic Arabidopsis than in Col. and *PRI-GFP* transgenic Arabidopsis (third column). The pseudo-color scale on the right indicates the intensity of the fluorescence, in which yellow and red represent the minimum and maximum intensity, respectively. Scale bar = 10 μm. G, Quantification of the luminal pH in the vacuoles of Col., *PRI-GFP*, *AtPAP1-GFP-1*, *AtPAP1-GFP-2*, and *AtPAP1-D Arabidopsis*. Error bars represent SE of 30 measurements from 10 different intact vacuoles. In B, C, D, E, and G, data are shown as the mean ± SE, which were analyzed based on more than 20 seedlings. Statistical significance was determined using Student's *t* test in different Arabidopsis lines. n.s., $P > 0.01$; *$P < 0.01$; **$P < 0\ 0.001$.

by previous findings that mutations of the seven pH loci result in a high petal pH and a shift of the flower color to blue in *petunia* and morning glory (de Vlaming et al., 1983; Fukada-Tanaka et al., 2000; Ohnishi et al., 2005). In grapevines, *VvMYB5a* and *VvMYB5b*, which are *pH4* orthologs, are involved in the regulation of vacuolar acidification and partially in the flavonoid pathway (Cavallini et al., 2013). Our work also indicates that MdMYB1/10 directly activates MATE-LIKE and ABC transporters for anthocyanin accumulation in the vacuole (Fig. 5, B and E). Therefore, enhanced accumulation of anthocyanins in red-flesh fruits (Fig. 4A; Supplemental Fig. S11C), red-leaf apple seedlings (Supplemental Fig. S10B), and transgenic calli and fruits overexpressing *MdMYB1* (Fig. 3D; Supplemental Fig. S8B) results from both the direct regulation of MdMYB1/10 on *MATE-LIKE* and *ABC transporter* and indirect effects on the vacuolar transport of anthocyanins via vacuolar acidification.

In addition, It was found in this study that most of the MdMYB1 binding sites are around or < 1 kb far from the transcription start of those target genes such as *MdVHP1* ($-799 \sim -721$ bp). In contrast, MdMYB1 binds to a *MdVHA-B1 cis*-element which is > 2 kb far from the transcription start (Fig. 1A), just as several other TFs do (Maruyama-Nakashita et al., 2005; Behnam et al., 2013). In animal, a few TFs have binding sites that even lie beyond the > 10 kb of promoter sequence (Wang et al., 2007). For those TFs and their binding sites, the specific DNA three-dimensional structure may make the TFs close to the transcription start of target genes.

Molecular Mechanisms and Physiological Roles of the Coregulation of the Vacuolar Transport of Malate and Anthocyanins by MdMYB1

In apples, MdMYB1 is a crucial component of the MdMYB1-MdbHLH3-MdTTG1 complex, which acts as the master regulatory machinery for anthocyanin synthesis in controlling the coloration of apple fruit peels and flesh (Takos et al., 2006; Espley et al., 2007; Ban et al., 2007; An et al., 2012; Xie et al., 2012). As the target genes of MdMYB1 TF, anthocyanin structural genes, such as *MdDFR* and *MdUFGT*, contain MYB cis-elements in their promoters. Both MdMYB1 and MdbHLH3/33 physically bind to these cis-elements to activate the expression of these genes (An et al., 2012; Xie et al., 2012). Interestingly, our data show that MYB cis-elements are present in the promoters of many genes encoding vacuolar proton pumps and anthocyanin transporters. Among these genes, *MdVHA-B1*, *MdVHA-B2*, *MdVHA-E2*, *MdVHP1*, *MdMATE-LIKE1*, and *ABC transporter* are the direct target genes of MdMYB1 TF (Fig. 5E). In addition, the overexpression of *MdbHLH3* enhances the expression of *MdVHA-B1* and *MdVHA-B2*, leading to lower pH values in apple plants (Supplemental Fig. S5, A and C). However, EMSA showed that MdbHLH3 did not directly bind to the promoters of *MdVHA-Bs* (data not shown), suggesting that MdbHLH3 enhances the expression of the *MdVHA-Bs* and vacuolar acidification in an indirect way. Therefore, the apple MdTTG1-MdbHLH3-MdMYB1 complex is an important regulatory machinery that modulates not only anthocyanin synthesis but also the activities of V-ATPase and V-PPase and the vacuolar transport of anthocyanins, demonstrating the multiple functions of MdMYB1 in the acidification and coloration of plant organs, such as fruits and flowers. From a physiological perspective, it makes sense that the synthesis and the vacuolar transport of anthocyanins are regulated by the same machinery to prevent any detrimental effect of anthocyanin accumulation in the cytosol on cell metabolism.

In addition to regulating anthocyanin synthesis and vacuolar transport, our data, including RNA-Seq analysis, showed that MdMYB1 directly binds to the promoter of malate transporter *MdtDT* to transcriptionally

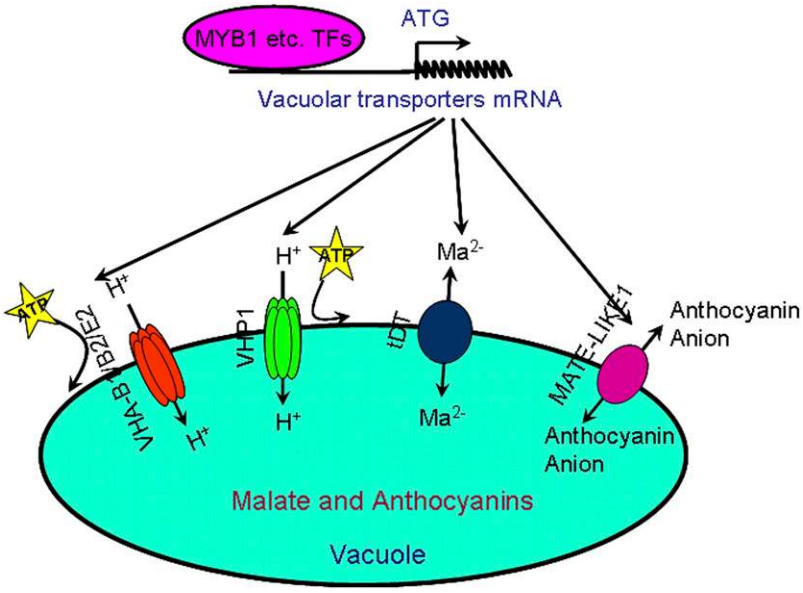

Figure 7. A model of the MYB TF that transcriptionally activates proton pumps and secondary transporters in modulating pH and the accumulation of malate and anthocyanins in the vacuole of plants.

activate its expression in apple calli (Fig. 5, D and E; Supplemental Table S1 and Supplemental Appendix S2). We also found that vacuolar acidification resulting from the overexpression of *MdVHA-B1* alone leads to elevated malate levels in apple calli (Fig. 3G) and tobacco flowers (Supplemental Fig. S9D). It is interesting that the overexpression of subunit *MdVHA-B1* also increases the expression of *MdtDT* in apple calli (Supplemental Fig. S13). Therefore, both the direct regulation and indirect regulation (via vacuolar acidification) of vacuolar malate transport by MdMYB1 converge at the transcriptional activation of *MdtDT*, thereby increasing malate levels in red-flesh apples compared to non-red-flesh apples (Fig. 4E; Supplemental Fig. S11F) and in apple calli overexpressing *MdMYB1* (Fig. 3G). Considering that malate and anthocyanins are two different types of metabolites stored in the vacuole, it is tempting to ask what advantage, if any, the coregulation of the vacuolar transport of malate and anthocyanins by MdMYB1 confers on cell function. Based on the fundamental role of malate synthesis, degradation and transport in cell pH control (Kurkdjian and Guern, 1989; Hurth et al., 2005; Martinoia et al., 2007), we propose that this coregulation helps to maintain pH homeostasis in the cytosol of plants where MdMYB1 is expressed. When both V-ATPase and V-PPase are up-regulated by MdMYB1, vacuolar acidification is enhanced (Fig. 3, H and I), and corresponding alkalization of the cytosol is expected. It has been shown that the alkalization of the cytosol up-regulates malate synthesis and its subsequent transport into the vacuole, generating protons to maintain the pH of the cytosol (Gout et al., 1992, 1993). In this scenario, the direct transcriptional activation of *MdtDT* coupled with indirect up-regulation of *MdtDT* transcript levels by way of vacuolar acidification/cytosol alkalization would be most effective in transporting newly synthesized malate into the vacuole. The fact that the cells in apple calli overexpressing *MdMYB1* or *MdVHA-B1* (Fig. 3J) have higher buffering capacity but a relatively lower cellular pH (Fig. 3, H and I) supports this hypothesis. However, the mechanism by which *MdtDT* expression is up-regulated by vacuolar acidification/cytosol alkalinization is not clear. In Arabidopsis, *tDT* is up-regulated by both malate feeding (Emmerlich et al., 2003) and the acidification of the cytosol in leaf mesophyll cells (Hurth et al., 2005).

The alleles *MdMYB10* and *AtPAP1-D* constitutively express transcripts throughout the entire apple plant and Arabidopsis, thereby producing high levels of anthocyanins in all of the organs (Espley et al., 2007; Li et al., 2012; Qiu et al., 2014). We demonstrated that these alleles also activate vacuolar proton pumps as well as anthocyanin and malate transporters. As a result, plants with MdMYB10 and AtPAP1-D loci have higher malate content and lower pH values (Fig. 4, E–G; Fig. 6, E–G). In apples, however, the differences in malate content between the red-flesh and non-red-flesh fruits are much less obvious in the ripe fruits at 120 d after flowering than in the young ones at 90 d after flowering (Fig. 4E). Espley et al. (2013) also report that the overexpression of *MdMYB10* cDNA has little influence on the malate content in the ripe fruits at 130 DAB in the transgenic Royal Gala apple. The cause for the reduced effect of MdMYB10 on malate levels in ripe fruits is not clear, but is likely related to the fruit ripening process. Because *MdALMT9*, the most likely candidate gene for *Ma* in apples (Bai et al., 2012), is not a target gene of MdMYB1 (Fig. 5E), nor is its expression up-regulated by vacuolar acidification in apple calli overexpressing *MdVHA-B1* (Supplemental Fig. S13) and red-flesh apples (Fig. 5D), it is possible that *MdALMT9* plays a larger role in determining malate levels in ripe fruits. This phenomenon, however, is not restricted to red-flesh fruits in apples. Ectopic expression of *MdMDH* and *MdVHP1* remarkably enhances the malate content in young fruits but has little impact on ripe fruits in transgenic tomatoes (Yao et al., 2011a; 2011b). Obviously, further work is needed to understand the regulatory network for controlling malate levels during the fruit-ripening process.

Agricultural Significance and Potential Application of These Findings

Color is one of the most eye-catching traits, not only for ornamental plants (Obón and Rivera, 2006; Młodzińska, 2009) but also for edible crops. In edible plant organs, such as fleshy fruits, anthocyanin and associated polyphenolics are beneficial to human health, while acidity contributes to taste and flavor. These metabolites largely determine the dietary and market values of these economic crops (Butelli et al., 2008; Sweetman et al., 2009; Etienne et al., 2013). Therefore, these characteristics are major targets of breeding programs for these edible crops. Our work clearly demonstrates that the master regulators for anthocyanin synthesis, MdMYB1/10 and AtPAP1, also transcriptionally activate proton pumps and secondary transporters in modulating cellular pH and vacuolar accumulation of anthocyanins and malate (Fig. 7). For apples, this regulation leads to alterations in fruit color and acidity, two important traits for fruit quality. These findings may be useful in developing novel biotechnological strategies, as well as in informing traditional breeding programs in the creation of new cultivars with improved color, taste, and flavor.

MATERIAL AND METHODS

Plant Materials and Growth Conditions

The apple calli used in this study were induced from the young embryos of Orin apples (*Malus domestica* Borkh.). They were grown on MS medium supplemented with 0.5 mg L^{-1} indole-3-acetic acid (IAA) and 1.5 mg L^{-1} 6-benzylaminopurine (6-BA) at 25°C in the dark. The calli were subcultured three times at 15-d intervals before being used for genetic transformation and in other assays.

The apple fruits used for injection of viral vectors were collected from mature trees of the cultivar Red Delicious grown in a commercial orchard near Tai-An City. Fruits were bagged at 35 DAB. The bagged fruits were harvested at 140 DAB and were de-bagged before injection.

For sexual crossing, a red-fleshed apple B9, which contains a heterozygous *MdMYB10* locus, was used as a pollen donor, while another red-flesh apple, YL, having a heterozygous *MdMYB10* locus, was the maternal parent. The resultant hybrid population was comprised of 80 red-flesh and 48 non-red-flesh trees. These trees were grown in a field at an experimental farm. Among them, five red hybrid trees and five green ones produced fruits with similar fruit development and ripening stages. The red-flesh fruits from five red hybrid trees and non-red-flesh fruits from five green trees were harvested at different developmental stages. Red-flesh and non-red-flesh fruits were mixed to eliminate genetic differences and used for further investigation. To further eliminate genetic differences to the greatest extent, another hybrid population from a sexual cross between a red-flesh apple, "Jinshanyilamu," and a non-red-flesh apple, "Yepinguo," which contains 30 hybrid trees bearing red-flesh fruits and 30 trees bearing non-red-flesh fruits, was used. The fruits were harvested at 90 DAB. Subsequently, the red-flesh and non-red-flesh fruits of 30 trees were mixed for further investigation.

The Arabidopsis (*Arabidopsis thaliana*) ecotype Columbia, PAP1 gain-of-function mutant *PAP1-D*, and two *35S::PAP1-GFP* transgenic lines, *PAP1-GFP-1* and *PAP1-GFP-2*, were used. After being treated at 4°C for 3 d, the seeds were sown on MS medium. The plants were grown at 21°C in a 16-h light period (200 μmol m^{-2} s^{-1}). Tobacco (*Nicotiana tabacum*) was cultivated in a growth room at 25°C using natural light with a daylight extension of 14 h.

Genetic Transformation and the Construction of the Expression Vectors

To construct *MdMYB1* and *MdVHA-B1* sense (S) overexpression and antisense (AS) suppression vectors, the full-length cDNAs of *MdMYB1* and *MdVHA-B1*, a specific fragment of *MdMYB1* and a conserved fragment of *MdVHA-B1* and *MdVHA-B2* were isolated from Gala apples using RT-PCR. All cDNAs were digested with *Eco*RI/*Bam*HI and cloned into pRI plant transformation vectors downstream of CaMV *35S* promoters. All primers used are listed in Supplemental Table S2.

Meanwhile, the full-length cDNAs of *Arabidopsis PAP1* and *PAP2* were amplified from Arabidopsis ecotype Columbia (Col 0) using RT-PCR. The resulting cDNAs were digested with *Eco*RI/*Bam*HI and cloned into pRI-GFP plant transformation vectors downstream of CaMV *35S* promoters. The primers used are listed in Supplemental Table S2.

For apple calli transformation, the recombinant plasmids, including MdMYB1-S, MdVHAB1-S, MdMYB1-S+MdVHAB1-S, MdMYB1-S+MdVHABs-AS, MdMYB1-AS, MdVHABs-AS and MdMYB1-AS+MdVHABs-AS, were introduced into Orin apple calli using an *Agrobacterium*-mediated method, as described by Horsch et al. (1985) and Li et al. (2012). The resultant transgenic apple calli were grown on MS medium supplemented with 0.5 mg L^{-1} indole-3-acetic acid (IAA) and 1.5 mg L^{-1} 6-benzylaminopurine (6-BA) at 25°C in the dark. Subsequently, the wild type and these seven transgenic apple calli were placed under 25°C plus UVB light conditions for two weeks, before for further investigation.

For tobacco transformation, the recombinant plasmids *MdMYB1-S* and *MdVHAB1-S* were introduced into *Agrobacterium tumefaciens* strain LBA4404. Tobacco was transformed with LBA4404 using a leaf disc method (Horsch et al., 1985).

For Arabidopsis transformation, the *PAP1-GFP* recombinant plasmid was introduced into wild type (Col 0) via *Agrobacterium* strain GV3101 using a floral dip method (Clough and Bent, 1998). The seeds of the transgenic plants were individually harvested and subsequently shelfed. Homozygous transgenic lines were used for further investigation.

RNA Extraction, RT-PCR, and qRT-PCR Assays

RNA extraction, as well as RT-PCR and qRT-PCR assays, were performed with the methods described by Hu et al. (2015). For all of the analyses, the signal obtained for a gene of interest was normalized against the signal obtained for the *18S* gene (Defilippi et al., 2005). All of the samples were tested in three to four biological replicates. All of the primers used for the semiquantitative RT-PCR and qRT-PCR are listed in Supplemental Tables S2 and S3.

RNA-Seq analysis

Total RNA was extracted from the fruits of the red- or non-red-flesh hybrid trees at 90 DAB. Subsequently, the RNAs for the red and non-red-fleshed fruits were used to construct libraries for high-throughput parallel sequencing using an Illumina genome analyzer II. A rigorous algorithm was used to identify the differentially expressed genes in these samples. A 1% false discovery rate was set to measure the threshold of the *P*-value in our tests and analyses by manipulating the FDR value (Audic and Claverie, 1997). $P < 0.001$ and the absolute value of log2Ratio > 1 were used as the threshold to determine the significance of the gene expression differences, according to Audic and Claverie (1997). A GO analysis was used to predict gene function and calculate the functional category distribution frequency.

Chromatin Immunoprecipitation qPCR Analysis

35S::MdMYB1-GFP and *35S::GFP* transgenic apple calli were used for the ChIP-qPCR analysis. The anti-GFP antibody (Beyotime) was used for chromatin immunoprecipitation (ChIP), as described by Xie et al. (2012). The resultant samples were used as templates for qPCR. The primers used for ChIP-PCR are listed in Supplemental Table S4.

EMSA

EMSA was conducted according to Xie et al. (2012). *MdMYB1* was cloned into the expression vector *pGEX4T-1*. The MdMYB1-GST recombinant protein was expressed in *Escherichia coli* strain BL21 and purified using glutathione Sepharose beads (Thermo Scientific). An oligonucleotide probe of the *MdMYB1* promoter was labeled using an EMSA probe biotin labeling kit (Beyotime) according to the manufacturer's instructions. The recombined protein of MdMYB1-GST was incubated with 10× binding buffer, 1 μg/μL poly (dI-dC), and 400 fmol of biotin-labeled double-stranded binding consensus oligonucleotides (total volume 20 μL) using a LightShift Chemiluminescent EMSA Kit (Thermo Scientific). The binding reaction was performed at room temperature for 20 min. The DNA-protein complexes were separated on 6.5% nondenaturing polyacrylamide gels, electrotransferred, and detected following the manufacturer's instructions. The binding specificity was also examined by competition with a fold excess of unlabeled oligonucleotides. The primers used for EMSA are listed in Supplemental Table S5.

Transient Expression Assays

Transient expression assays were conducted using apple calli. The promoters of *MdVHA-B1*, *MdVHA-B2*, and *MdVHA-B3* were cloned into *PBI121-GUS* to fuse with the reporter gene GUS. The resultant recombinant plasmids $P_{MdVHAB1}$::*GUS*, $P_{MdVHAB2}$::*GUS*, and $P_{MdVHAB3}$::*GUS* were genetically introduced into Orin apple calli via an *agrobacterium*-mediated method. Subsequently, *35S::MdMYB1* transformant was cotransformed into the above-mentioned transgenic calli. Finally, histochemical staining was performed to detect GUS activity in the transgenic calli, as described by Xie et al. (2012).

Enzyme Extraction and V-ATPase Activity Assays

The isolation of the tonoplast membranes assays were performed as described by Terrier et al. (2001). Bafilomycin A_1-sensitive ATP hydrolysis of vacuolar membranes was assayed by measuring the production of inorganic phosphate, as described by Lu et al. (2002). Meanwhile, proton transport activity of V-ATPase was measured by ATP-dependent fluorescent quenching of the pH-sensitive fluorescent probe acridine orange (Lu et al., 2002).

Construction of Transient Expression Vectors in Apple Fruits

To construct the antisense expression viral vectors, the *MdMYB1* cDNA fragment and conserved *MdVHA-Bs* fragment were amplified with RT-PCR using apple fruit cDNA as the template. The PCR products were cloned into the tobacco rattle virus (TRV) vector in the antisense orientation under the control of the dual *35S* promoter. The resultant vectors were named TRV-MdMYB1 and TRV-MdVHABs. Subsequently, they were introduced into *Agrobacterium tumefaciens* strain GV3101 by electrical shock. The transformants were then used for apple fruit infiltrations.

To generate the overexpression viral vectors, full-length cDNAs of *MdMYB1* and *MdVHA-B1* were inserted into the IL-60 vector under the control of the *35S* promoter. The resultant vector plasmids were named MdMYB1-IL and MdVHAB1-IL, and then their single or recombined plasmids were used for apple fruit infiltrations. Fruit infiltrations were performed as described by Li et al. (2012).

DNA-Affinity Trapping of DNA-Binding Proteins

DNA promoter fragments of the *MdVHA-B1* containing MYB cis-elements were used to isolate the proteins binding to the cis-elements in these promoter fragments. The biotinylated DNA promoter fragments were generated by PCR using the primers that are listed in Supplemental Table S4. Nuclear protein extracts for EMSA were prepared from Red Delicious apple plants that were grown under natural conditions. The biotinylated DNA promoter fragment was immobilized on Dynabeads M-280 streptavidin (Invitrogen) according to the manufacturer's instructions, in which 2 mg of beads were immobilized using 2× binding buffer (10 mM Tris-HCl, pH 7.5, 1 mM EDTA, and 2 M NaCl). The binding of the protein to the DNA was performed as described by Gabrielsen et al. (1989), with some modifications. A 15-min incubation at 25°C was performed after the beads were resuspended in protein binding buffer (20 mM Tris-HCl, pH 8.0, 1 mM EDTA, 10% (v/v) glycerol, 100 mM NaCl, 0.05% (v/v) Triton X-100, and 1 mM DTT) and mixed with apple nuclear protein extracts. The Dynabeads were washed three times with protein-binding buffer before the proteins were eluted in elution buffer (20 mM Tris-HCl, pH 8.0, 1 mM EDTA, 10% (v/v) glycerol, 1 M NaCl, 0.05% (v/v) Triton X -100, and 1 mM DTT). The protein digestion, mass spectrometry, and data analysis were performed as described by Shaikhali et al. (2012).

Measurement of Vacuolar pH

Vacuolar pH of apple calli protoplasts was monitored with the cell-permeant and pH-sensitive fluorescent dye BCECF-AM (Tang et al., 2012). Vacuolar pH value was quantified by a ratio analysis of the pH-dependent (488 nm) and pH-independent (458 nm) excitation wavelengths from a calibration curve (Supplemental Fig. S7), and ratio images were produced using the ion concentration tool of Zeiss LSM confocal software.

pH Buffering Capacity

The pH buffering capacity of the experimental material was measured using a pH electrode (Rex Instruments; E-201-C) and an ORP electrode (ORP-412, Cany Precision Instruments), as described by Florou-Paneri et al. (2001). A 10-g sample was placed in a beaker, and 100 mL of distilled water was added. The mixture was stirred for approximately 30 min and was subsequently titrated with 0.1 M NaOH, with continuous stirring, to decrease the pH by one unit. The amount of NaOH consumption was used to express the pH buffering capacity of the samples.

Determination of the Total Anthocyanin Content

Total anthocyanins were extracted using a methanol-HCl method and detected as described by Lee and Wicker (1991).

Determination of the Malate Content

Malate content was measured by HPLC, as described by Hu et al. (2015).

Statistical Analysis

Samples were analyzed in triplicate, and the data were expressed as the mean ± SD unless noted otherwise. Statistical significance was determined using Student's *t* test. A difference with $P \leq 0.01$ was considered significant, and a difference with $P \leq 0.001$ was extremely significant.

Supplemental Data

Supplemental Figure S1. Analysis of the three deduced isoforms of apple V-ATPase subunit B.

Supplemental Figure S2. The recombinant MdMYB1 does not bind to the promoter region of the *MdVHA-B3* gene in the electrophoretic mobility shift assays (EMSAs).

Supplemental Figure S3. MdMYB1 activates the *MdVHA-B1* and *MdVHA-B2* but not *MdVHA-B3* promoters as detected by GUS assays.

Supplemental Figure S4. Analysis of protein abundance of MdMYB1, MdVHA-B1, MdVHA-B2, and MdVHA-B3 in transgenic apple calli lines with western blotting.

Supplemental Figure S5. MdbHLH3 activates *MdMYB1*, *MdVHA-B1*, and *MdVHA-B2* to increase malate content in transgenic apple plants.

Supplemental Figure S6. Characterization of the purity of protoplasts, vacuoles, and tonoplast vesicles isolated from WT apple plants.

Supplemental Figure S7. In situ calibration of BCECF-AM in protoplast vacuoles.

Supplemental Figure S8. Transient expression of MdMYB1 and MdVHA-B1 via the viral vector-based transformation alters the coloration and acidity of apple fruits and petals.

Supplemental Figure S9. The ectopic expression of MdMYB1 and MdVHA-B1 promotes acidity and coloration in transgenic tobacco flowers.

Supplemental Figure S10. The phenotype differences between the red-leaf and green-leaf apple hybrids in a sexually crossed population (YL×B9).

Supplemental Figure S11. The phenotype differences between red-flesh and non-red-flesh genotypes in a hybridization population from 'Jinshanyilamu X 'Yepingguo'.

Supplemental Figure S12. The relative expression level of the V-ATPase subunit genes in MdVHAB1-Sac and WT apple calli (relative transcripts = MdVHAB1-Sac transcripts/WT transcripts).

Supplemental Figure S13. The relative expression levels of *MdtDT*, *MdALMT9*, *MdMATE-LIKE1*, *MdMATE-LIKE2*, *MdMATE-LIKE3*, and *ABC transporter* in wild-type (WT) and *MdVHA-B1* transgenic apple calli.

Supplemental Table S1. The transcriptional changes of the anthocyanin- and malate-related genes in red-flesh versus non-red-flesh apple fruits with RNA-seq.

Supplemental Table S2. List of primers used for real-time PCR.

Supplemental Table S3. List of primers used for real-time quantitative PCR.

Supplemental Table S4. List of primers used for ChIP-PCR.

Supplemental Table S5. List of primers used for EMSA.

Supplemental Appendix 1. The identified proteins that bind to MYB cis-element of MdVHA-B1 promoter in LC/MS data.

Supplemental Appendix 2. The relative expression folds of the detected genes in red-flesh versus non-red-flesh apple fruits with RNA-seq assay.

Supplemental Appendix 3. Amino acid sequence alignment of putative MATE and ABC transporters of Arabidopsis and apple.

ACKNOWLEDGMENTS

We thank Prof. Ilan Sela of Hebrew University of Jerusalem, Israel, for IL-60-BS binary vectors and Prof. Takaya Moriguchi of National Institute of Fruit Tree Science, Japan, for Orin apple calli.

Received August 25, 2015; accepted December 4, 2015; published December 4, 2015.

LITERATURE CITED

Albert NW, Lewis DH, Zhang H, Schwinn KE, Jameson PE, Davies KM (2011) Members of an R2R3-MYB transcription factor family in Petunia are developmentally and environmentally regulated to control complex floral and vegetative pigmentation patterning. Plant J **65:** 771–784

Allan AC, Hellens RP, Laing WA (2008) MYB transcription factors that colour our fruit. Trends Plant Sci **13:** 99–102

An XH, Tian Y, Chen KQ, Wang XF, Hao YJ (2012) The apple WD40 protein MdTTG1 interacts with bHLH but not MYB proteins to regulate anthocyanin accumulation. J Plant Physiol **169:** 710–717

An XH, Tian Y, Chen KQ, Liu XJ, Liu DD, Xie XB, Cheng CG, Cong PH, Hao YJ (2015) *MdMYB9* and *MdMYB11* are involved in the regulation of the JA-induced biosynthesis of anthocyanin and proanthocyanidin in apples. Plant Cell Physiol **56:** 650–662

Audic S, Claverie JM (1997) The significance of digital gene expression profiles. Genome Res **7:** 986–995

Bai Y, Dougherty L, Li M, Fazio G, Cheng L, Xu K (2012) A natural mutation-led truncation in one of the two aluminum-activated malate transporter-like genes at the *Ma* locus is associated with low fruit acidity in apple. Mol Genet Genomics **287:** 663–678

Ballester AR, Molthoff J, de Vos R, Hekkert Bt, Orzaez D, Fernández-Moreno JP, Tripodi P, Grandillo S, Martin C, Heldens J, et al (2010) Biochemical and molecular analysis of pink tomatoes: deregulated expression of the gene encoding transcription factor SlMYB12 leads to pink tomato fruit color. Plant Physiol **152:** 71–84

Ban Y, Honda C, Hatsuyama Y, Igarashi M, Bessho H, Moriguchi T (2007) Isolation and functional analysis of a MYB transcription factor gene that is a key regulator for the development of red coloration in apple skin. Plant Cell Physiol **48:** 958–970

Behnam B, Iuchi S, Fujita M, Fujita Y, Takasaki H, Osakabe Y, Yamaguchi-Shinozaki K, Kobayashi M, Shinozaki K (2013) Characterization of the promoter region of an *Arabidopsis* gene for 9-*cis*-epoxycarotenoid dioxygenase involved in dehydration-inducible transcription. DNA Res **20:** 315–324

Butelli E, Titta L, Giorgio M, Mock HP, Matros A, Peterek S, Schijlen EG, Hall RD, Bovy AG, Luo J, Martin C (2008) Enrichment of tomato fruit with health-promoting anthocyanins by expression of select transcription factors. Nat Biotechnol **26:** 1301–1308

Cao ZH, Zhang SZ, Wang RK, Zhang RF, Hao YJ (2013) Genome wide analysis of the apple MYB transcription factor family allows the identification of *MdoMYB121* gene confering abiotic stress tolerance in plants. PLoS One **8:** e69955

Cavallini E, Zenoni S, Finezzo L, Guzzo F, Zamboni A, Avesani L, Tornielli GB (2013) Functional diversification of grapevine MYB5a and MYB5b in the control of flavonoid biosynthesis in a petunia anthocyanin regulatory mutant. Plant Cell Physiol **55:** 517–534

Clough SJ, Bent AF (1998) Floral dip: a simplified method for *Agrobacterium*-mediated transformation of *Arabidopsis thaliana.* Plant J **16:** 735–743

Keenan Curtis K, Kane PM (2002) Novel vacuolar H^+-ATPase complexes resulting from overproduction of Vma5p and Vma13p. J Biol Chem **277:** 2716–2724

de Vlaming P, Schram AW, Wiering H (1983) Genes affecting flower colour and pH of flower limb homogenates in *Petunia hybrida*. Theor Appl Genet **66:** 271–278

Debeaujon I, Peeters AJ, Léon-Kloosterziel KM, Koornneef M (2001) The TRANSPARENT TESTA12 gene of *Arabidopsis* encodes a multidrug secondary transporter-like protein required for flavonoid sequestration in vacuoles of the seed coat endothelium. Plant Cell **13:** 853–871

Defilippi BG, Kader AA, Dandekar AM (2005) Apple aroma: alcohol acyltransferase, a rate limiting step for ester biosynthesis, is regulated by ethylene. Plant Sci **168:** 1199–1210

Emmerlich V, Linka N, Reinhold T, Hurth MA, Traub M, Martinoia E, Neuhaus HE (2003) The plant homolog to the human sodium/dicarboxylic cotransporter is the vacuolar malate carrier. Proc Natl Acad Sci USA **100:** 11122–11126

Etienne A, Génard M, Lobit P, Mbeguié-A-Mbéguié D, Bugaud C (2013) What controls fleshy fruit acidity? A review of malate and citrate accumulation in fruit cells. J Exp Bot **64:** 1451–1469

Espley RV, Hellens RP, Putterill J, Stevenson DE, Kutty-Amma S, Allan AC (2007) Red colouration in apple fruit is due to the activity of the MYB transcription factor, *MdMYB10.* Plant J **49:** 414–427

Espley RV, Brendolise C, Chagné D, Kutty-Amma S, Green S, Volz R, Putterill J, Schouten HJ, Gardiner SE, Hellens RP, Allan AC (2009) Multiple repeats of a promoter segment causes transcription factor autoregulation in red apples. Plant Cell **21:** 168–183

Espley VR, Bovy A, Bava C, Allan CA (2013) Analysis of genetically modified red-fleshed apples reveals effects on growth and consumer attributes. Plant Biotechnol J **11:** 408–419

Faraco M, Spelt C, Bliek M, Verweij W, Hoshino A, Espen L, Prinsi B, Jaarsma R, Tarhan E, de Boer AH, et al (2014) Hyperacidification of vacuoles by the combined action of two different P-ATPases in the tonoplast determines flower color. Cell Reports **6:** 32–43

Fernie AR, Martinoia E (2009) Malate. Jack of all trades or master of a few? Phytochemistry **70:** 828–832

Florou-Paneri P, Christaki E, Botsoglou NA, Kalousis A, Spois AB (2001) Performance of broilers and the hydrogen ion concentration in their digestive tract following feeding of diets with different buffering capacities. Arch Geflugelkd **65:** 236

Francisco RM, Regalado A, Ageorges A, Burla BJ, Bassin B, Eisenach C, Zarrouk O, Vialet S, Marlin T, Chaves MM, Martinoia E, Nagy R (2013) ABCC1, an ATP binding cassette protein from grape berry, transports anthocyanidin 3-O-Glucosides. Plant Cell **25:** 1840–1854

Fukada-Tanaka S, Inagaki Y, Yamaguchi T, Saito N, Iida S (2000) Colour-enhancing protein in blue petals. Nature **407:** 581

Gabrielsen OS, Hornes E, Korsnes L, Ruet A, Oyen TB (1989) Magnetic DNA affinity purification of yeast transcription factor tau–a new purification principle for the ultrarapid isolation of near homogeneous factor. Nucleic Acids Res **17:** 6253–6267

Gaxiola RA, Palmgren MG, Schumacher K (2007) Plant proton pumps. FEBS Lett **581:** 2204–2214

Gomez C, Terrier N, Torregrosa L, Vialet S, Fournier-Level A, Verriès C, Souquet JM, Mazauric JP, Klein M, Cheynier V, Ageorges A (2009) Grapevine MATE-type proteins act as vacuolar H^+-dependent acylated anthocyanin transporters. Plant Physiol **150:** 402–415

Goodman CD, Casati P, Walbot V (2004) A multidrug resistance-associated protein involved in anthocyanin transport in Zea mays. Plant Cell **16:** 1812–1826

Gout E, Bligny R, Douce R (1992) Regulation of intracellular pH values in higher plant cells. Carbon-13 and phosphorus-31 nuclear magnetic resonance studies. J Biol Chem **267:** 13903–13909

Gout E, Bligny R, Pascal N, Douce R (1993) 13C nuclear magnetic resonance studies of malate and citrate synthesis and compartmentation in higher plant cells. J Biol Chem **268:** 3986–3992

Horsch RB, Fry JE, Hoffmann NL, Wallroth M, Eichholtz D, Rogers SG (1985) A simple and general method for transferring genes into plants. Science **227:** 1229–1231

Hu DG, Ma QJ, Sun CH, Sun MH, You CX, Hao YJ (2015) Overexpression of *MdSOS2L1*, an CIPK protein kinase, improves the antioxidant metabolites to enhance salt tolerance in apple and tomato. Physiol Plant

Hurth MA, Suh SJ, Kretzschmar T, Geis T, Bregante M, Gambale F, Martinoia E, Neuhaus HE (2005) Impaired pH homeostasis in Arabidopsis lacking the vacuolar dicarboxylate transporter and analysis of carboxylic acid transport across the tonoplast. Plant Physiol **137:** 901–910

Koes R, Verweij W, Quattrocchio F (2005) Flavonoids: a colorful model for the regulation and evolution of biochemical pathways. Trends Plant Sci **10:** 236–242

Kovermann P, Meyer S, Hörtensteiner S, Picco C, Scholz-Starke J, Ravera S, Lee Y, Martinoia E (2007) The *Arabidopsis* vacuolar malate channel is a member of the ALMT family. Plant J **52:** 1169–1180

Kurkdjian A, Guern J (1989) Intracellular pH: measurement and importance in cell activity. Annu Rev Plant Physiol Plant Mol Biol **40:** 271–303

Lee HS, Wicker L (1991) Anthocyanin pigments in the skin of lychee fruit. J Food Sci **56:** 466–468

Li YY, Mao K, Zhao C, Zhao XY, Zhang HL, Shu HR, Hao YJ (2012) MdCOP1 ubiquitin E3 ligases interact with MdMYB1 to regulate light-induced anthocyanin biosynthesis and red fruit coloration in apple. Plant Physiol **160:** 1011–1022

Lin-Wang K, Bolitho K, Grafton K, Kortstee A, Karunairetnam S, McGhie TK, Espley RV, Hellens RP, Allan AC (2010) An R2R3 MYB transcription factor associated with regulation of the anthocyanin biosynthetic pathway in Rosaceae. BMC Plant Biol **10:** 50

Lobit P, Genard M, Soing P, Habib R (2006) Modelling malic acid accumulation in fruits: relationships with organic acids, potassium, and temperature. J Exp Bot **57:** 1471–1483

Lu M, Vergara S, Zhang L, Holliday LS, Aris J, Gluck SL (2002) The amino-terminal domain of the E subunit of vacuolar $H(^+)$-ATPase (V-ATPase) interacts with the H subunit and is required for V-ATPase function. J Biol Chem **277:** 38409–38415

Mahmoudi E, Soltani BM, Yadollahi A, Hosseini E (2012) Independence of color intensity variation in red flesh apples from the number of repeat units in promoter region of the *MdMYB10* gene as an allele to *MdMYB1* and *MdMYBA*. Iran J Biotechnol **10:** 153–160

Marinova K, Pourcel L, Weder B, Schwarz M, Barron D, Routaboul JM, Debeaujon I, Klein M (2007) The *Arabidopsis* MATE transporter TT12 acts as a vacuolar flavonoid/H^+-antiporter active in proanthocyanidin-accumulating cells of the seed coat. Plant Cell **19:** 2023–2038

Martinoia E, Maeshima M, Neuhaus HE (2007) Vacuolar transporters and their essential role in plant metabolism. J Exp Bot **58:** 83–102

Marty F (1999) Plant vacuoles. Plant Cell **11:** 587–600

Maruyama-Nakashita A, Nakamura Y, Watanabe-Takahashi A, Inoue E, Yamaya T, Takahashi H (2005) Identification of a novel *cis*-acting element conferring sulfur deficiency response in *Arabidopsis* roots. Plant J **42:** 305–314

Młodzińska E (2009) Survey of plant pigments: molecular and environmental determinants of plant colors. Acta Biol Cracov Ser; Bot **51:** 7–16

Obón C, Rivera D (2006) Plant Pigments and their manipulation. Econ Bot **60:** 92

Ohnishi M, Fukada-Tanaka S, Hoshino A, Takada J, Inagaki Y, Iida S (2005) Characterization of a novel Na^+/H^+ antiporter gene *InNHX2* and comparison of *InNHX2* with *InNHX1*, which is responsible for blue flower coloration by increasing the vacuolar pH in the Japanese morning glory. Plant Cell Physiol **46:** 259–267

Padmanaban S, Lin X, Perera I, Kawamura Y, Sze H (2004) Differential expression of vacuolar H^+-ATPase subunit c genes in tissues active in membrane trafficking and their roles in plant growth as revealed by RNAi. Plant Physiol **134:** 1514–1526

Palmgren MG (2001) Plant plasma membrane H^+-ATPases: powerhouses for nutrient uptake. Annu Rev Plant Physiol Plant Mol Biol **52:** 817–845

Palmgren MG, Nissen P (2011) P-type ATPases. Annu Rev Biophys **40:** 243–266

Qiu J, Sun S, Luo S, Zhang J, Xiao X, Zhang L, Wang F, Liu S (2014) *Arabidopsis AtPAP1* transcription factor induces anthocyanin production in transgenic *Taraxacum brevicorniculatum*. Plant Cell Rep **33:** 669–680

Quattrocchio F, Verweij W, Kroon A, Spelt C, Mol J, Koes R (2006) PH4 of *Petunia* is an R2R3 MYB protein that activates vacuolar acidification through interactions with basic-helix-loop-helix transcription factors of the anthocyanin pathway. Plant Cell **18:** 1274–1291

Quattrocchio FM, Spelt C, Koes R (2013) Transgenes and protein localization: myths and legends. Trends Plant Sci **18:** 473–476

Ramsay NA, Glover BJ (2005) MYB-bHLH-WD40 protein complex and the evolution of cellular diversity. Trends Plant Sci **10:** 63–70

Shaikhali J, de Dios Barajas-Lopéz J, Ötvös K, Kremnev D, Garcia AS, Srivastava V, Wingsle G, Bako L, Strand Å (2012) The CRYPTOCHROME1-dependent response to excess light is mediated through the transcriptional activators ZINC FINGER PROTEIN EXPRESSED IN INFLORESCENCE MERISTEM LIKE1 and ZML2 in *Arabidopsis*. Plant Cell **24:** 3009–3025

Shiratake K, Martinoia E (2007) Transporters in fruit vacuoles. Plant Biotechnol **24:** 127–133

Swanson SJ, Jones RL (1996) Gibberellic acid induces vacuolar acidification in barley aleurone. Plant Cell **8:** 2211–2221

Sweetman C, Deluc LG, Cramer GR, Ford CM, Soole KL (2009) Regulation of malate metabolism in grape berry and other developing fruits. Phytochemistry **70:** 1329–1344

Takos AM, Jaffé FW, Jacob SR, Bogs J, Robinson SP, Walker AR (2006) Light-induced expression of a MYB gene regulates anthocyanin biosynthesis in red apples. Plant Physiol **142:** 1216–1232

Tang RJ, Liu H, Yang Y, Yang L, Gao XS, Garcia VJ, Luan S, Zhang HX (2012) Tonoplast calcium sensors CBL2 and CBL3 control plant growth and ion homeostasis through regulating V-ATPase activity in *Arabidopsis*. Cell Res **22:** 1650–1665

Terrier N, Sauvage FX, Ageorges A, Romieu C (2001) Changes in acidity and in proton transport at the tonoplast of grape berries during development. Planta **213:** 20–28

Verweij W, Spelt C, Di Sansebastiano GP, Vermeer J, Reale L, Ferranti F, Koes R, Quattrocchio F (2008) An H^+ P-ATPase on the tonoplast determines vacuolar pH and flower colour. Nat Cell Biol **10:** 1456–1462

Vimolmangkang S, Han Y, Wei G, Korban SS (2013) An apple MYB transcription factor, MdMYB3, is involved in regulation of anthocyanin biosynthesis and flower development. BMC Plant Biol **13:** 176

Wang Q, Li W, Liu XS, Carroll JS, Jänne OA, Keeton EK, Chinnaiyan AM, Pienta KJ, Brown M (2007) A hierarchical network of transcription factors governs androgen receptor-dependent prostate cancer growth. Mol Cell **27:** 380–392

Xie XB, Li S, Zhang RF, Zhao J, Chen YC, Zhao Q, Yao YX, You CX, Zhang XS, Hao YJ (2012) The bHLH transcription factor MdbHLH3 promotes anthocyanin accumulation and fruit colouration in response to low temperature in apples. Plant Cell Environ **35:** 1884–1897

Xu KN, Wang A, Brown S (2012) Genetic characterization of the Malocus with pH and titratable acidity in apple. Mol Breed **30:** 899–912

Yao YX, Li M, Zhai H, You CX, Hao YJ (2011a) Isolation and characterization of an apple cytosolic malate dehydrogenase gene reveal its function in malate synthesis. J Plant Physiol **168:** 474–480

Yao YX, Dong QL, You CX, Zhai H, Hao YJ (2011b) Expression analysis and functional characterization of apple *MdVHP1* gene reveals its involvement in $Na^{(+)}$, malate and soluble sugar accumulation. Plant Physiol Biochem **49:** 1201–1208

Yoshida K, Mori M, Kondo T (2009) Blue flower color development by anthocyanins: from chemical structure to cell physiology. Nat Prod Rep **26:** 884–915

Zhao Q, Zhao YJ, Zhao BC, Ge RC, Li M, Shen YZ, Huang ZJ (2009) Cloning and functional analysis of wheat V-H^+-ATPase subunit genes. Plant Mol Biol **69:** 33–46